Evolution of conduction and interface states of laterally wet-oxidized AlGaAs with oxidation time

J. F. Chen, R. S. Hsiao, W. K. Hung, J. S. Wang, J. Y. Chi, H. C. Yu, and Y. K. Su

Citation: Journal of Applied Physics **99**, 023711 (2006); doi: 10.1063/1.2164532
View online: http://dx.doi.org/10.1063/1.2164532
View Table of Contents: http://scitation.aip.org/content/aip/journal/jap/99/2?ver=pdfcov
Published by the AIP Publishing

Evolution of conduction and interface states of laterally wet-oxidized AlGaAs with oxidation time

J. F. Chen,[a] R. S. Hsiao, and W. K. Hung
Department of Electrophysics, National Chiao Tung University, Hsinchu, Taiwan, Republic of China

J. S. Wang
Department of Physics, Chung Yuan Christian University, Chung-Li, Taiwan, Republic of China

J. Y. Chi
Industrial Technology Research Institute (OES/ITRI), Hsinchu, Taiwan, Republic of China

H. C. Yu and Y. K. Su
Institute of Microelectronic, Department of Electrical Engineering, National Cheng Kung University, Tainan, Taiwan, Republic of China

(Received 21 June 2005; accepted 6 December 2005; published online 27 January 2006)

The conduction and interface states of laterally wet-oxidized GaAs-AlGaAs-GaAs structures after various oxidation times are investigated. Effective current blocking is achieved after 150 min oxidation and the conduction of current through the oxidized AlGaAs layer is controlled by the Poole-Frenkel mechanism, from which a relative dielectric constant of 7.07 is obtained. At an oxidation time of 15 min, capacitance-voltage spectra exhibit capacitance dispersion over frequency, implying the presence of an interface state. The intensity of the dispersion increases with increasing the oxidation time and admittance spectroscopy reveals a significant interface state at ~0.28 eV at 45 min. Further increasing the oxidation time to 150 min broadens the interface state to a set of continuous interface states from 0.19–0.31 eV with decreasing densities from 3×10^{11} to 0.9×10^{11} eV^{-1} cm^{-2} and generates fixed charges of about 9.1×10^{11} cm^{-2} in the oxidized layer. By comparison to a similar trap in a relaxed InGaAs/GaAs, the interface state is tentatively assigned to the interaction of residual As with dislocations. © *2006 American Institute of Physics*. [DOI: 10.1063/1.2164532]

I. INTRODUCTION

Recently, the lateral wet oxidation of AlGaAs[1] has attracted considerable attention because it can be applied in distribution Bragg reflectors and current blocking layers in vertical cavity surface-emitting lasers (VCSELs).[2–4] Its high dielectric constant, high breakdown voltage, and low threshold voltage enable the wet-oxidized AlGaAs layer also to be used as an insulator gate in metal-oxide-semiconductor field effect transistors (MOSFETs).[6–8] However, the electrical properties of the oxidized AlGaAs layers are inferior to those of the SiO_2/Si structures. Numerous studies on the oxidation chemistry,[9] kinetics,[10,11] and microstructures[5,9,12–15] have been undertaken. The wet oxidation of AlGaAs has been shown to yield residual elemental As that degrades the electrical properties[9,13] in the layer and at the interface. Moreover, significant strain exists around the oxide/semiconductor interface because of volume shrinkage,[9] possibly forming defect traps. Despite the fact that the effect of an interfacial layer on the current-voltage characteristics has been theoretically studied by thermionic-emission theory,[16–19] including the nonequilibrium charging effect of interface states,[20,21] relatively little work has been done to establish experimentally the relationships among the current conduction, interface states,[22] and oxidation conditions. Therefore, this work systematically investigates the electrical properties of a GaAs-AlGaAs-GaAs capacitor with various oxidation times by current-voltage (*I-V*), capacitance-voltage (*C-V*), and admittance measurements.

II. EXPERIMENT

The studied samples were grown on n^+-GaAs (100) substrates by molecular beam epitaxy. An n^+-GaAs buffer layer was initially grown, followed by an *n*-GaAs (with Si doping of 10^{17} cm^{-3}) layer with a thickness of 0.3 μm and an undoped AlGaAs layer with a thickness of 0.1 μm. On top of the AlGaAs layer, an n^+-GaAs layer with a thickness of 0.1 μm was grown to terminate the growth process. The GaAs layers were grown at 600 °C at a growth rate of 2.78 Å/s and the AlGaAs layer was grown at 600 °C at an Al rate of 1.71 Å/s and a Ga rate of 0.035 Å/s. After the layer growth, a SiO_2 layer was deposited and patterned as a mask. Reactive ion etching was used to etch down to the bottom GaAs layer and expose the AlGaAs layer from the sides to avoid undesirable undercutting. Then, the samples were immediately placed in a furnace, fed by a water bubbler at 100 °C with N_2 carrier gas at a rate of 2 L/min. The samples were thus oxidized at 425 °C. This oxidation temperature was selected because a much lower oxidation temperature would not have been high enough to convert completely the AlGaAs to an oxidized layer and a much higher temperature would cause the oxidation to proceed beyond the AlGaAs/GaAs interface.[12] Following oxidation, another

[a]Electronic address: jfchen@cc.nctu.edu.tw

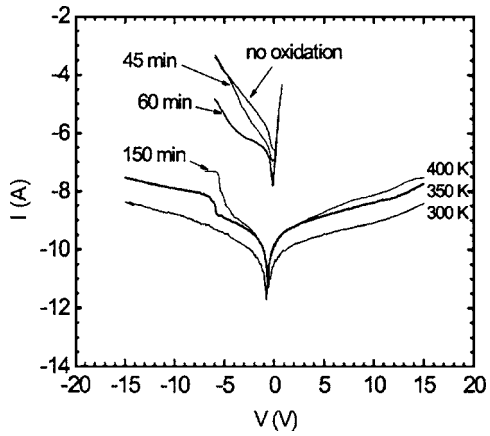

FIG. 1. 300 K *I-V* characteristics without oxidation and after 45, 60, and 150 min of oxidation. Effective current blocking is achieved after 150 min oxidation.

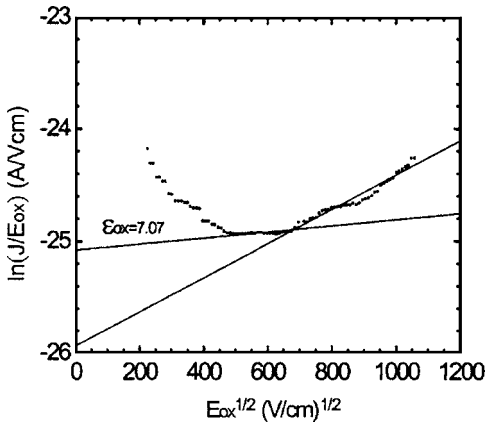

FIG. 2. Plot of $\ln(J/E_{ox})$ vs $E_{ox}^{1/2}$ from the reverse current-voltage characteristic after 150 min of oxidation. In the middle-field region, the curve is linear, and its slope yields a dielectric constant of 7.07, a value close to that of the oxidized layer, confirming a Poole–Frenkel emission.

SiO_2 layer was deposited on the sample edge to prevent the flow of leakage current. After the front SiO_2 layer had been removed, Ti/Au was evaporated and alloyed as the front contact. The back Ohmic contact was fabricated by depositing Au/Ge/Ni/Au. The *C-V* and admittance spectroscopy measurements were made using an HP4194A gain-phase analyzer.

III. RESULTS

A. Current-voltage characterizations

Figure 1 plots the 300 K *I-V* characteristics of the samples without and with 45, 60, and 150 min oxidation. The sample without oxidation exhibits some rectification because the bottom GaAs layer is slightly depleted. The reverse leakage current is as high as 0.1 mA at −5 V, indicating that the AlGaAs barrier is not sufficiently high to suppress the leakage current. An oxidation of 45 min only slightly suppressed the reverse current. Increasing the oxidation time to 60 min further suppressed the reverse current but did not significantly affect the forward current, implying that the oxidation time did not suffice. Effective current blocking can be achieved by increasing the oxidation time to 150 min, as shown by the symmetry of the *I-V* characteristics at a current of below 3 nA at ±15 V. This result shows that the AlGaAs layer is completely converted to an oxide layer.

When current is limited by the oxidized layer, the *I-V* characteristics are similar to those of semiconductor-insulator-semiconductor (*n-i-n*) structures. At low voltages, the current is caused mainly by the thermally generated carriers in the insulator, since the injection of electrons is strongly opposed by the high-energy barrier of the oxidized layer. As will be shown later, fixed charges are present in the oxidized layer. When the applied electric field is sufficiently large, the barrier height seen by the electrons trapped on the charge centers may be reduced, increasing the rate of Poole–Frenkel (PF) emission, which is given by[23]

$$J \propto \exp\left(\frac{q\beta_{\mathrm{PF}}}{2kT}E_{\mathrm{ox}}^{1/2}\right)E_{\mathrm{ox}},$$

where J is the current density; E_{ox} is the electric field in the oxidized layer, and $\beta_{PF}=q/\pi\varepsilon_o\varepsilon_{ox}$. Accordingly, $\ln(J/E_{ox})$ varies linearly with $E_{ox}^{1/2}$. Figure 2 plots $\ln(J/E_{ox})$ vs $E_{ox}^{1/2}$ for the reverse *I-V* curve at 300 K of the sample with 150 min oxidation. The data fall into three regions. In the low-field region where the slope is negative, the conduction does not obey PF emission since the electric field is not sufficiently large to slant the energy band. When the field is increased, the data fall in a linear region, the slope of the (solid) line yields a dielectric constant of 7.07, which is close to those previously obtained for the oxidized AlGaAs layers,[9,14] confirming PF emission. When the electric field is further increased, the data deviate from the PF emission, as evidenced by the stronger dependence on the electric field, perhaps because of phonon-assisted tunneling. This strong dependence on field produces a steep current rise. The dotted line in Fig. 2 shows that this large-field region starts at an electric field of 4.9×10^5 MV/cm ($E^{1/2}=700$ V/cm), which corresponds to an applied voltage of −8 V. This reverse voltage is comparable to the value at which the reverse current (at 350 K) increases sharply, as shown in Fig. 1.

B. Capacitance-voltage characteristics

Figures 3(a)–3(c) plot the capacitance-voltage (*C-V*) spectra at 300 K for samples without and with 45 and 60 min of oxidation, respectively. In the case without oxidation, the weak dependence on voltage reflects a small depletion of the bottom GaAs layer. According to the parallel-capacitor model, the capacitance is consistent with the thickness of the AlGaAs layer. Outside the voltage range of interest, the capacitance decreases as the voltage increases because the leakage current increases ($>10^{-5}$ A), implying that the AlGaAs barrier is not sufficiently high to enable the applied voltage to deplete the bottom GaAs layer. This characteristic is typical of a GaAs/AlGaAs/GaAs structure. The independence of the capacitance on frequency suggests the absence of appreciable interface states.

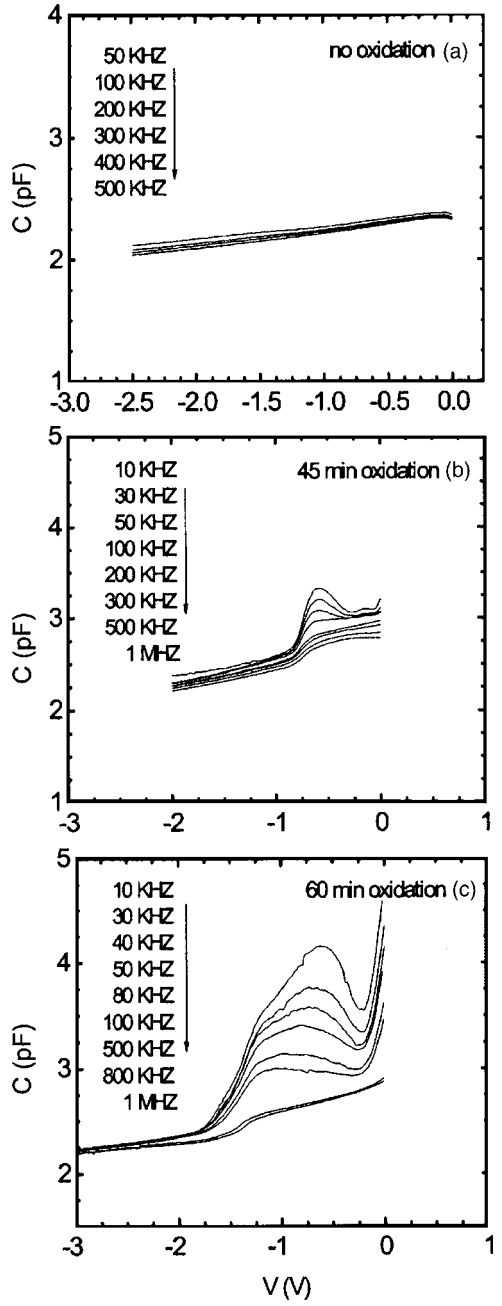

FIG. 3. 300 K capacitance-voltage spectra (a) without oxidation, (b) after 45, and (c) after 60 min oxidation. Without oxidation, capacitance is nearly independent of voltage and frequency. After oxidation, the capacitance displays frequency dispersion because an interface state is formed.

After 45 min of oxidation, the capacitance exhibits a stronger dependence on voltage, as shown in Fig. 3(b), reflecting the depletion of the bottom GaAs layer. The zero-voltage capacitance exceeds that of the sample without oxidation because oxidation increases the dielectric constant of the AlGaAs layer. The capacitance depends significantly on frequency at voltages of around −0.7 V, whose dependence is characteristic of the presence of an interface state. A negative dc voltage moves the Fermi level downward and depletes the bottom GaAs layer. When the Fermi level intersects with the interface state, additional capacitance arises at low frequency when the interface state can respond to an ac voltage. As the applied voltage moves the Fermi level away from the interface state, the contribution from the interface state is diminished and the low-frequency capacitance approaches the high-frequency capacitance. This result shows that the density of the interface state is not sufficiently large to pin the Fermi level.

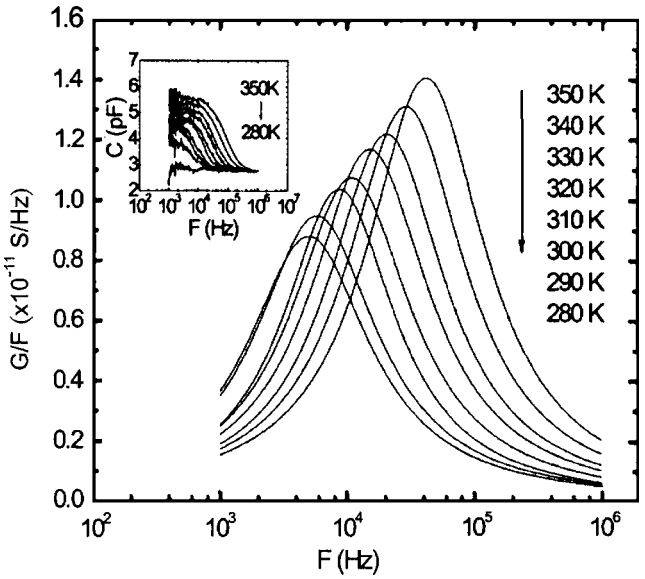

FIG. 4. Temperature-dependent G/F-F spectra at −0.5 V and corresponding C-F spectra in the inset, after 60 min of oxidation. The G/F peaks yield an activation energy of 0.28 eV.

C. Admittance spectroscopy

When the oxidation time is increased to 60 min, the capacitance dispersion becomes more pronounced and the zero-bias capacitance markedly increases, as shown in Fig. 3(c). From the low-frequency zero-bias capacitance of 4.6 pF, and the oxide thickness of 0.093 μm, determined by scanning electron micrography (SEM), the dielectric constant is estimated to be 7.82, whose value is comparable to that obtained from the I-V characteristics after 150 min of oxidation. Admittance spectroscopy was performed on this sample to determine the emission time of the interface state. Figure 4 shows the temperature-dependent conductance/frequency-frequency (G/F-F) spectra at −0.5 V, and the corresponding capacitance-frequency (C-F) spectra in the inset. The G/F-F spectra peak when the measuring frequency is comparable to the emission rate of the interface state. The dependence of the inflection frequency on temperature yields an activation energy (capture cross section) of 0.28 eV (9.19×10^{-17} cm^{-2}), plotted as solid diamonds in Fig. 5. This activation energy slightly increases to 0.29 eV (3.21×10^{-16} cm^{-2}) as the voltage is increased to −0.2 V. This nearly constant activation energy suggests that the interface state is likely a single level.

As the oxidation time is further increased to 150 min, the C-V curve saturated at both positive and negative voltages, as shown in Fig. 6(a). The C-V spectra exhibit accumulation, depletion and inversion regions from right to left. The accumulation capacitance of 5.1 pF and the oxide thickness of 0.093 μm yield a dielectric constant to be 7.69, which is close to that obtained from the sample oxidized by

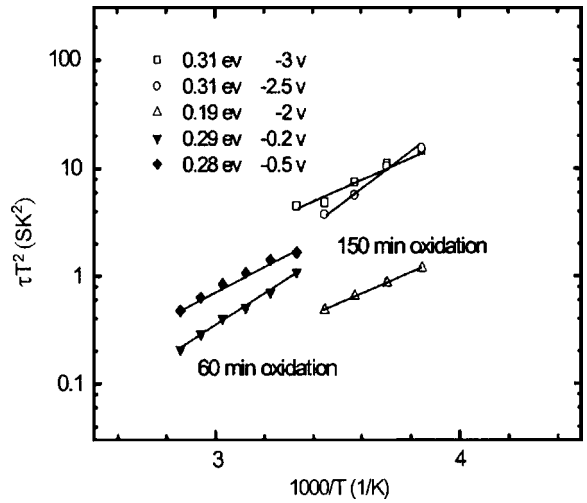

FIG. 5. Arrhenius plots of the emission times of the interface states after 60 min (solid points) and 150 min oxidation (hollow points). After 60 min of oxidation, the activation energy increases from 0.28 to 0.29 eV as the voltage decreases from −0.5 to −0.2 V. After 150 min of oxidation, the activation energy increases from 0.19 to 0.31 eV as the voltage decreases from −2 to −3 V.

60 min and is within the range from 4.5 to 8.4 reported for Al_2O_3 by Ashby *et al.*[13] The capacitance of ~4 pF in the inversion region is close to a theoretically predicted value of 3.6 pF at the onset of inversion. Interestingly, the *C-V* curve after 150 min of oxidation exhibits a significant parallel shift to the left by about 3 V, relative to the 60 min oxidation, suggesting the presence of fixed oxide charges. A simple calculation reveals that the flat-band capacitance is 4.67 pF and the fixed oxide charges have a density of 9.1×10^{11} cm^{-2}, as shown in Fig. 6(a). This value is about one or two orders of magnitude greater than that observed in SiO_2, probably because the sample did not undergo annealing.

The nearly constant difference between the high- and low-frequency capacitance in the depletion region, as shown in Fig. 6(a), suggests the presence of continuous interface states, rather than a single level. The plots of G/F spectra versus voltage, as shown in Fig. 6(b), reveal a peak at a voltage corresponding to the depletion region. This peak arises when the Fermi level intersects with the probed interface states. The emission times of the interface states are obtained from the temperature-dependent G/F vs F curves at −2.5 V, as plotted in Fig. 6(c). Each curve exhibits a peak, which shifts to higher frequency as the temperature increases, reflecting a short emission time at high temperature, from which an activation energy can be obtained. Figure 5 shows the Arrhenius plots of the emission times obtained at various voltages from −2 to −3 V (hollow points). The activation energy (capture cross section) increases from 0.19 (7.9×10^{-18} cm^2) to 0.31 eV (1.07×10^{-16} cm^2) as the voltage decreases from −2 to −3 V. This broad range of activation energy confirms the continuity of interface states, and the fact that the emission time increases as the reverse voltage decreases is consistent with a longer emission time for deeper interface states. From the amplitude of the conductance peak, the density of the interface states is estimated to be 3×10^{11} eV^{-1} cm^{-2} at $E_c - 0.19$ eV, decreasing to 0.9×10^{11} eV^{-1} cm^{-2} at $E_c - 0.31$ eV.

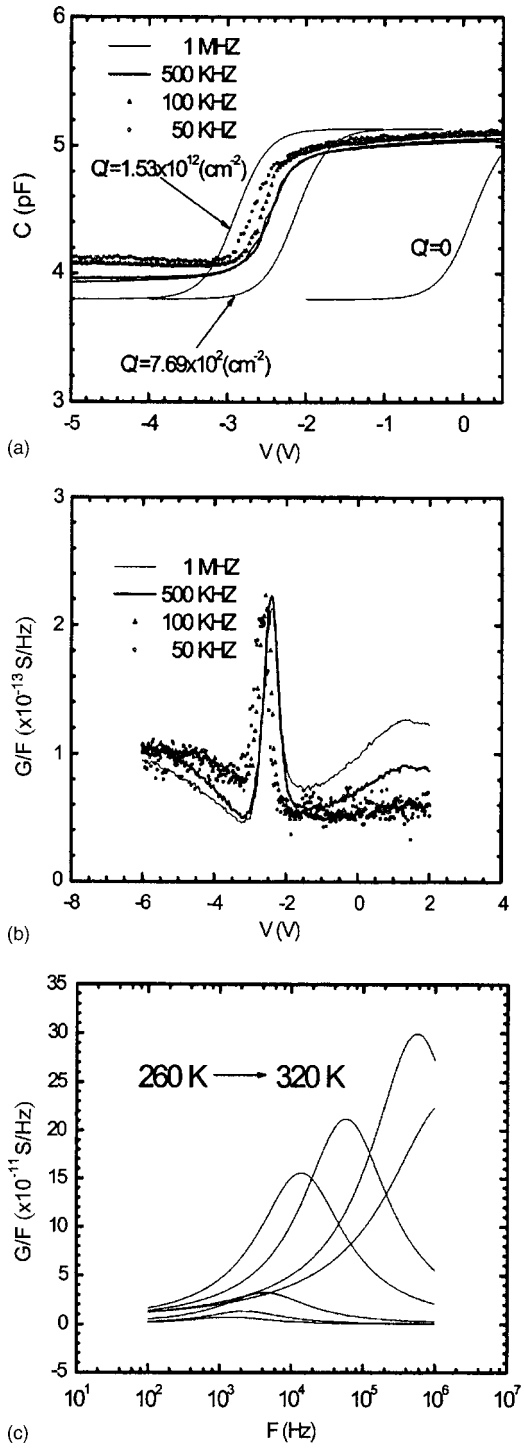

FIG. 6. (a) *C-V*, (b) *G/F-V*, and (c) *G/F-F* spectra after 150 min of oxidation. The parallel shift in the *C-V* curve indicates the presence of fixed oxide charges with a density of about 9.1×10^{11} cm^{-2}; the constant difference between the high- and low-frequency capacitance in the depletion region suggests continuous interface states whose emission times are obtained from the *G/F-F* spectra in (c). Figure 5 presents the corresponding results.

Consider the origin of the interface state at 0.28–0.29 eV formed by oxidation. The interface state has a similar activation energy to one of the traps previously observed by Tzeng *et al.*[22] by measuring the low-frequency

noise in wet-oxidized AlAs. Ashby *et al.*[15] observed residual elemental As in the vicinity of the oxide interface by transmission electron microscopy (TEM) and Raman spectroscopy of oxidized AlGaAs peaks; they thus proposed that the Fermi level is pinned to the residual As precipitates. However, under As-rich conditions, such as when GaAs is grown by molecular beam epitaxy (MBE) at low temperatures, an EL2-like trap[24] near the midgap, generally considered an As antisite (As_{Ga}) or its complex, is often observed. This EL2-like trap has an activation energy that considerably exceeds the interface state observed here. A comparison with previous results suggests that, as well as the residual As element, lattice relaxation or strain may also be involved in the formation of the interface state. This interface state is similar to the trap (at ~0.3 eV) observed in a N-implanted GaAs after thermal annealing.[25] The implantation-induced trap broadens to a continuous band (ranging from 0.2 to 0.3 eV) as the N implantation dose increases, just as the interface state broadens with oxidation time. The N-implantation trap[25] was related to the implantation-induced lattice expansion because high-temperature annealing reduced the concentration of the traps and the lattice expansion. Therefore, the trap may be related to the lattice expansion. A similar trap at around 0.3 eV was observed in the vicinity of a relaxed InGaAs/GaAs interface,[26] where TEM revealed relaxation-induced misfit dislocations.[27] When relaxation occurs in the InGaAs/GaAs interface, strain energy can be relieved by removing atoms from the compressive InGaAs layer to the tensile GaAs layer. Ashby *et al.*[15] proposed that the As element is a volatile species during the oxidation. Therefore, the transferring species may be the As element, probably in the form of interstitial As_i or antisite As_{Ga} in the GaAs. This residual As, after interacting with the misfit dislocations, may form the observed interface state. Therefore, we tentatively suggest that the interface state is associated with the interaction between residual As and dislocations.

IV. CONCLUSIONS

The conduction and interface states of a laterally wet-oxidized AlGaAs layer in a GaAs/AlGaAs/GaAs capacitor are investigated. Effective current blocking is achieved after 150 min of oxidation, and the conduction through the oxidized AlGaAs layer can be explained by Poole–Frenkel emission. The oxidation introduces interface states that cause capacitance dispersion over frequency, whose intensity increases with oxidation time. Admittance spectroscopy reveals an interface state at 0.28 eV after oxidation for 60 min. Further increasing the oxidation time generates fixed charges with a density of about 9.1×10^{11} cm^{-2} in the oxidized layer and broadens the interface state to a continuous band from 0.19 to 0.31 eV, and the density decreases from 3×10^{11} to 0.9×10^{11} eV^{-1} cm^{-2}. A comparison with previous results suggests that the interface state is associated with the interaction between residual As and dislocations.

ACKNOWLEDGMENT

The authors would like to thank the National Science Council of the Republic of China, Taiwan for financially supporting this research under Contract No. NSC-93-2112-M-009-002.

[1] J. M. Dallesasse and N. Holonyak, Jr., A. R. Sugg, T. A. Richard, and N. El-Zein, Appl. Phys. Lett. **57**, 2844 (1990).
[2] D. L. Huffaker, D. G. Deppe, K. Kumar, and T. J. Rogers, Appl. Phys. Lett. **65**, 97 (1994).
[3] K. D. Choquette, R. P. Schneider, Jr., K. L. Lear, and K. M. Geib, Electron. Lett. **30**, 2043 (1994).
[4] K. L. Lear, K. D. Choquette, R. P. Schneider, Jr., S. P. Kilcoyne, and K. M. Geib, Electron. Lett. **31**, 208 (1995).
[5] R. D. Twesten, D. M. Follstaedt, K. D. Choquette, and R. P. Schneider, Jr., Appl. Phys. Lett. **69**, 19 (1996).
[6] E. I. Chen, N. Holonyak, Jr., and S. A. Maranowski, Appl. Phys. Lett. **66**, 2688 (1995).
[7] P. A. Parikh, S. S. Shi, J. Ibettson, E. L. Hu, and U. K. Mishra, Electron. Lett. **32**, 1724 (1996).
[8] E. F. Yu, J. Shen, M. Walther, T. C. Lee, and R. Zhang, Electron. Lett. **36**, 359 (2000).
[9] K. D. Choquette, K. M. Geib, C. I. H. Ashby, R. D. Twesten, O. Blum, H. Q. Hou, D. M. Follstaedt, B. E. Hammons, D. Mathes, and R. Hull, IEEE J. Sel. Top. Quantum Electron. **3**, 916 (1997).
[10] H. Nickel, J. Appl. Phys. **78**, 5201 (1995).
[11] M. Ochiai, G. E. Giudice, H. Temkin, J. W. Scott, and T. M. Cockerill, Appl. Phys. Lett. **68**, 1898 (1996).
[12] Y. S. Lee, Y. H. Lee, and J. H. Lee, Appl. Phys. Lett. **65**, 2717 (1994).
[13] C. I. H. Ashby, J. P. Sullivan, K. D. Choquette, K. M. Geib, and H. Q. Hou, J. Appl. Phys. **82**, 3134 (1997).
[14] E. F. Schubert, M. Passlack, M. Hong, J. Mannerts, R. L. Opila, L. N. Pfeiffer, K. W. Weat, C. G. Bethea, and G. J. Zydzik, Appl. Phys. Lett. **64**, 2976 (1994).
[15] C. I. H. Ashby, J. P. Sullivan, P. P. Newcomer, N. A. Missert, H. Q. Hou, B. E. Hammons, M. J. Hafich, and A. G. Baca, Appl. Phys. Lett. **70**, 2443 (1997).
[16] J. Bardeen, Phys. Rev. **71**, 717 (1947).
[17] C. R. Crowell and S. M. Sze, Solid-State Electron. **8**, 979 (1965).
[18] W. Shockley and W. T. Read, Phys. Rev. **87**, 835 (1952).
[19] H. T. Tseng and C. Y. Wu, Solid-State Electron. **30**, 383 (1987).
[20] H. C. Card and E. H. Roderick, J. Phys. D **4**, 1589 (1971).
[21] G. Gomila and J. M. Rubi, J. Appl. Phys. **81**, 2674 (1997).
[22] S. Y. Tzeng, M. J. Cich, R. Zhao, H. Feick, and E. R. Weber, Appl. Phys. Lett. **82**, 1063 (2003).
[23] S. M. Sze, in *Physics of Semiconductor Devices* (Wiley, New York, 1981), p. 402.
[24] J. F. Chen, N. C. Chen, S. Y. Chiu, P. Y. Wang, W. I. Lee, and A. Chin, J. Appl. Phys. **79**, 8488 (1996).
[25] J. F. Chen, J. S. Wang, M. M. Huang, and N. C. Chen, Appl. Phys. Lett. **76**, 2283 (2000).
[26] J. F. Chen, P. Y. Wang, J. S. Wang, C. Y. Tsai, and N. C. Chen, J. Appl. Phys. **87**, 1369 (2000).
[27] J. F. Chen, P. Y. Wang, J. S. Wang, N. C. Chen, X. J. Guo, and Y. F. Chen, J. Appl. Phys. **87**, 1251 (2000).